Battery Research by Means of Atomic Force Microscopy

Relevant for: Battery, Energy storage, Electrical properties, Conductive AFM, Surface roughness, Atomic force microscope

Atomic force microscopy enables better understanding of the structure of electrodes for lithium ion batteries. Localized electrical properties and the surface topography were investigated and are shown to be very useful for optimized key performance indicators like high rate capability and capacity retention

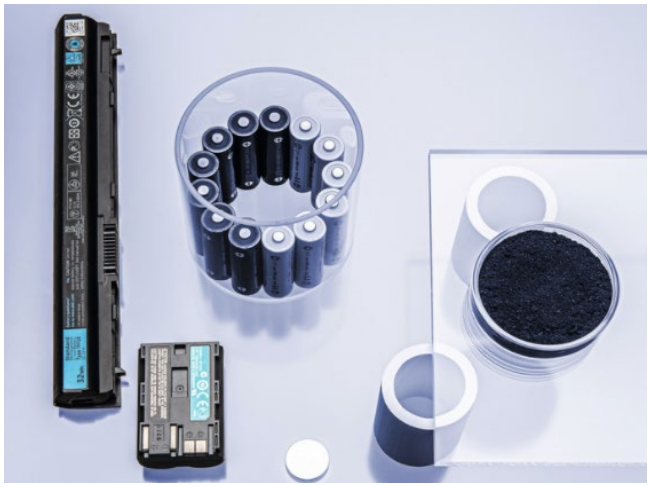

1 Introduction

In recent years, a lot of efforts were made to increase the energy density, the power density as well as the cycle lifetime of lithium ion batteries to meet the growing demand for storage devices for mobile and stationary applications[1]. Herein, the focus is mainly set to the development of new materials like electrochemically active materials for the cathode[2]–[4] and the anode[5]–[7], binders[8]–[10] or current collectors[11],[12]. However, the electrochemical properties of an electrode are not only determined by the components itself, but also by their processing[13]–[15] or by the electrode formulation[16].

In this work we show the influence of the amount of carbon black on the structure and the electrochemical properties of $LiFePO_4$ electrodes. On one hand, the content of additives should be as low as possible to yield a high energy density. On the other hand, the content of additives should be as high as necessary to ensure the functionality of the battery electrode.

Generally, carbon black serves as conductive additive in battery electrodes to enhance the electron transport between the electrochemically active particles. The aim of the study was to investigate how much carbon black is essential to realize high rate capable $LiFePO_4$ cathodes. For this purpose, $LiFePO_4$ electrodes with 0, 2, 5 and 10 wt% carbon black were prepared. The structure as well as the local electrical conductivity of the corresponding electrodes were investigated by atomic force microscopy. Finally, the electrodes were analyzed electrochemically.

2 Experimental

Atomic force microscopy investigations were performed by Tosca 400 AFM from Anton Paar. Tapping mode was used for topographic investigations using an AP-Arrow NCR cantilever with a typical resonance frequency of 285 kHz and a spring constant of 42 N/m. Conductive atomic force microscopy (C-AFM) was employed for measurement of local electrical properties using an AP-Arrow EFM cantilever with a typical resonance frequency of 75 kHz and a spring constant of 2.8 N/m. The cantilever is coated with an electrically conductive coating of Pt/Ir. C-AFM detects the current between tip and sample due to the applied constant voltage. The applied voltage ranged from 10 - 500 mV. The experiments were done in ambient atmosphere and supported by an active anti-vibration isolation table and an acoustic enclosure. Both components minimize external sources of noise and are part of the recommended setup of Tosca series AFM by Anton Paar. The investigated samples were cathodes for lithium ion batteries composed of commercially available lithium iron phosphate (LFP, particle size is in the submicron range) as electrochemically active material, polyacrylic acid (PAA, Alfa Aesar®, 25 wt% solution in water) as binder and carbon black (CB, Super-P Li™, Timcal) as conductive additive. The amount of binder was kept constant and the ratio between LFP and CB was varied.

Firstly, PAA was dissolved in a solvent mixture composed of 80 wt% ultrapure water and 20 wt% analytical grade ethanol. Subsequently, carbon black was added and the mixture was sonicated for 5 minutes. After addition of LFP the suspension was

homogenized by means of ultrasound for 2 minutes and of a turbo mixer for 1 h. The resulting slurries were cast on aluminum foil (Alujet, thickness: 30 µm) by using an adjustable doctor blade (film width: 50 mm). Afterwards, the electrodes were pre-dried for 8 h at a temperature of 90 °C under vacuum. Finally, circular electrodes with a diameter of 12 mm were laser-cut and dried at 90 °C for 24 h under vacuum. The final electrodes were amounted to LFP (95, 93, 90 and 85 wt%), carbon black (0, 2, 5 and 10 wt%) and binder (5 wt%). The average mass loading of LFP was between 1.7 and 1.8 mg cm^{-2}.

Electrochemical measurements were carried out using Swagelok®-type three electrode cells. Lithium foil served as counter and reference electrode. Polypropylene fleeces soaked with electrolyte were used as separator. The electrolyte was a solution of 1 M $LiPF_6$ in ethylene carbonate and dimethyl carbonate (1/1, *m/m*). The cells were assembled in an argon-filled glove box. Cycling experiments were performed with a Basytec CTS Lab XL battery tester. These experiments were carried out in the range of 2.8 and 3.8 V versus Li/Li^+, applying various currents which corresponds to C rates between 1/20 and 16. The cycling experiments were carried out as triple determination and the average values of the capacities are shown as representative results.

3 Results and Discussion

3.1 Local electrical conductivity

C-AFM detects the current between the tip and the surface for every measured location, i.e. pixel.

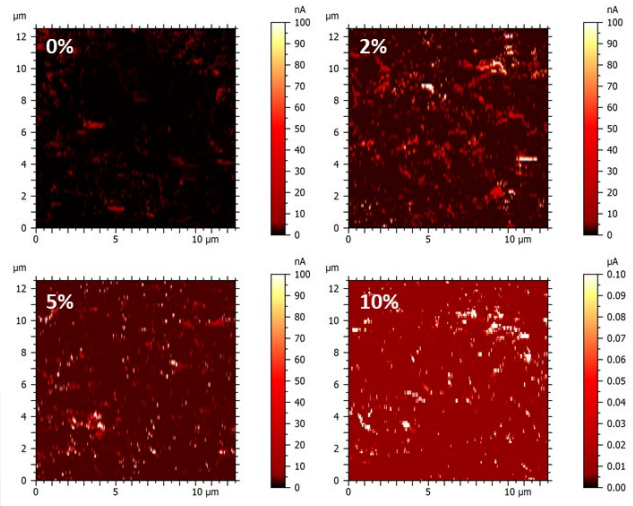

Figure 1 Current mapping by C-AFM measurements of cathode layers with increasing content of carbon black (0, 2, 5, 10%) at 10 mV bias voltage.

Consequently, the acquired data can be used to create current maps that show the lateral distribution of the electrical conductivity. Figure 1 shows the results of C-AFM measurements on the 4 cathode layers with increasing content of carbon black in the functional layer from 0 to 10%. The results show increasing detected current with increasing content of carbon black. The color scale indicates that the basic conductivity of the surface as well as the current flow of highly conductive locations (current peaks) within one dataset increases significantly when the content of carbon black is increased from 0 to 10%. Figure 2 shows the maximum detected current as a function of carbon black amount and bias voltage. The maximum current is the highest detected current value within the acquired dataset of 16000 pixels.

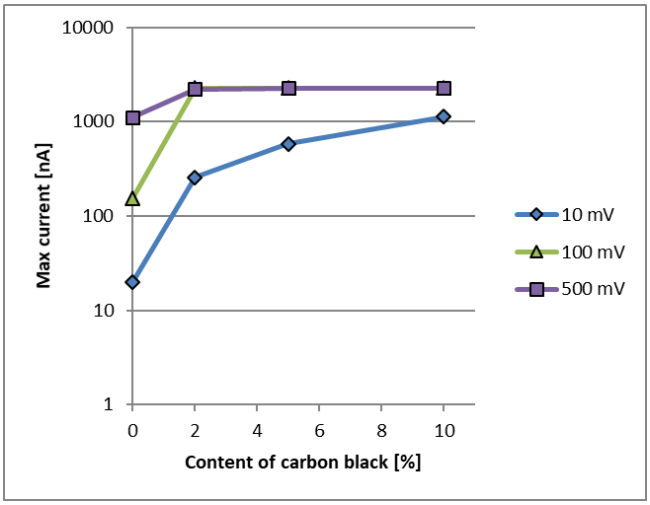

Figure 2 Maximum detected current as a function of content of carbon black and bias voltage. Higher content of carbon black significantly increases the detected current. The plateau for higher bias voltages and carbon black amount is caused by saturation of the current sensor.

As mentioned, the current significantly increases with increasing content of carbon black and bias voltage. It is important to note, that the observed saturation of the current for higher carbon black content and bias voltage is an effect of the current sensor, which has a maximum detectable current of 2200 nA. The same is observed for the mean detected current (see Fig. 3), which is calculated as the mean value of all detected pixels with a current higher than 1 nA. This is done by the “particle analysis” package of the Tosca analysis software.

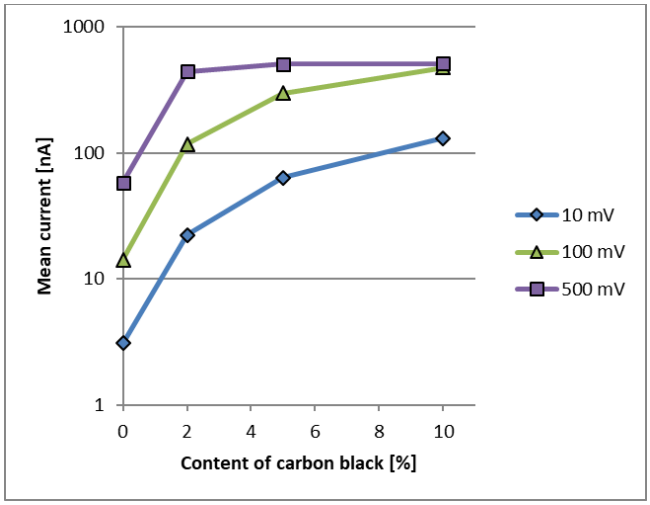

Figure 3 Mean detected current as a function of the amount of carbon black and the bias voltage. Higher content of carbon black significantly increases the current values.

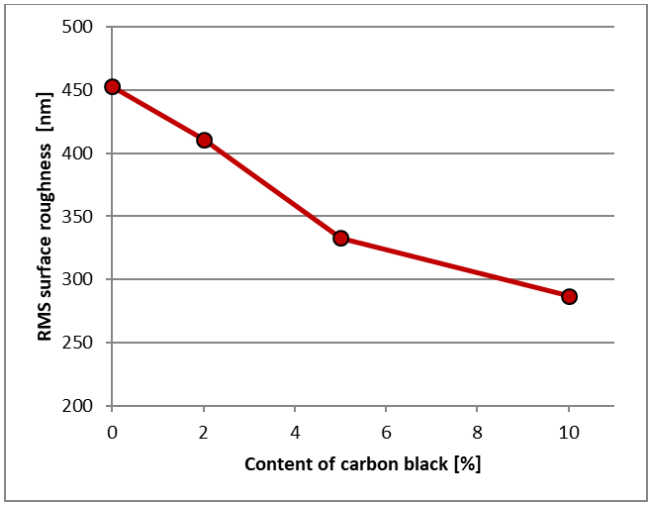

Figure 5 Surface roughness as a function of content of carbon black. The root mean square (RMS) roughness significantly decreases with increase of carbon black content.

3.2 Surface roughness

The coating, which is formed by aggregates/ agglomerates of different particles as a direct consequence of the manufacturing process results in a surface with high roughness. Such surfaces can be challenging for AFM systems with limited Z-range. Tosca 400 has a specified Z-range of 15 µm, making it the perfect tool for topographic investigations of rough surfaces.

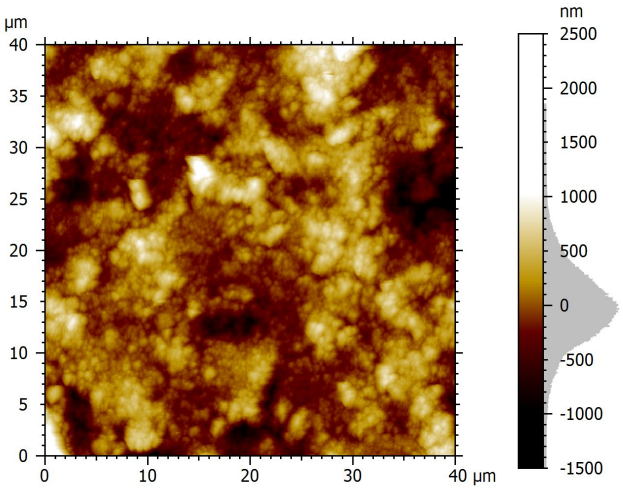

Figure 4 Height image of the sample with 5% carbon black acquired by tapping mode. The surface shows a granular structure with high roughness and aggregates/ agglomerates of particles.

Topographic AFM analysis yields a 3-dimensional model of the surface, with XYZ coordinates for every measured pixel. The surface roughness can be directly calculated from the gained data. RMS height Sq according to ISO 25178 represents the standard deviation of the Z-coordinate and is one of the most widely used parameters to describe surface roughness. Figure 5 shows the result of RMS surface roughness as a function of the content of carbon black.The results show a decreasing surface roughness with increasing content of carbon black. This can be explained by the difference in particle size between the LFP powder and carbon black. The primary particle size of carbon black (50 – 100 nm)[17] is much smaller than that of LFP (submicron range) , thus the carbon black is filling inter-granular gaps, voids or pores which leads to generally smoother surfaces.

3.3 Electrochemical characterization

The cycling test started with a formation sequence at low C rates (1/20 up to 1/2), followed by a stability test over 75 cycles applying 1 C which is shown in Figure 7. Finally, the high rate capability up to 16 C was investigated (Figure 6). In general, the capacity decreases with increased applied current (C rate) which can be explained by the limited lithium ion and electron diffusion rates in LFP[18],[19]. Up to 1 C no significant capacity differences depending on the amount of carbon black are observed. However, the lowest capacity is obtained for the sample without carbon black whereupon the effect becomes more prominent with increasing C rate. The capacity difference is most obvious at 16 C whereupon the sample with 10 wt% carbon black reaches the highest capacity. Thus, it can be concluded that the electrical connection of the particles does not significantly limit the capacity at moderate C rates (up to 1 C). However, by applying C rates up to 16 C, the capacity of the electrodes is more and more dominated by the electrical particle connection.

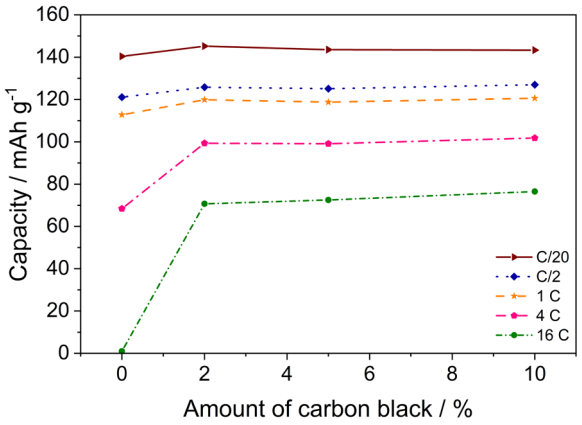

Figure 6 Capacity of LFP electrodes depending on the amount of carbon black and the applied current (C rate)

Hence, a direct correlation between the AFM measurements and the electrochemistry is found. The sample with the lowest surface roughness and the highest local electrical conductivity shows the highest capacity at a high applied current of 16 C. Independent of the amount of carbon black, the capacity is slightly increased within 75 cycles for all samples. It can be assumed that the electrode structure is slightly changed. Possibly more pores within the electrode are generated or the wetting with electrolyte is enhanced during cycling so that all parts of the electrode are reached during cell operation.

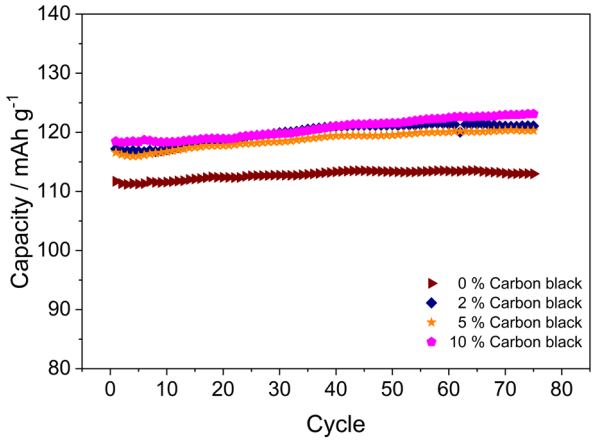

Figure 7: Capacity retention recorded at 1 C of LFP electrodes depending on the amount of carbon black.

As a matter of fact, the lowest capacity is observed for the sample without carbon black. However, by increasing the carbon amount from 2 to 10 wt% no difference in the available capacity is obtained.

Finally, it can be concluded that the capacity retention of the corresponding electrodes is not affected by the amount of carbon black.

4 Summary

Atomic force microscope Tosca 400 has been successfully used to investigate the topography and the electrical properties of LFP electrodes on the microscale. The results show, that increasing content of carbon black in LFP electrodes enhances the electrical conductivity which can be understood by a better electrical contact between the LFP particles as well as to the current collector by the addition of carbon black. The surface roughness decreases with higher carbon black contents which can be understood by the smaller particle size of carbon black, effectively filling gaps, voids and pores between the functional particles.

The results can be directly correlated with the electrochemical characterization of the LFP electrodes. The higher the local electrical conductivity and the lower the surface roughness the higher is the capacity at a high applied current of 16 C. The optimum amount of carbon black is between 5 and 10 wt%.

To conclude, atomic force microcopy is a powerful and efficient tool to correlate the structure of battery electrodes with their electrochemical properties. In contrast to other methods like scanning electron microscopy, atomic force microscopy enables to quickly investigate large areas of up to 100x100 µm in ambient environment. Hence, this method is also suitable for quality assurance for battery electrodes.

5 Acknowledgements

We would like to thank Prof. Dr. Hartmut Wiggers (Nanomaterial synthesis) and Prof. Dr. Doris Segets (Nanoprocessing) from the Institute for combustion and gas dynamics (IVG), University Duisburg-Essen for the collaboration and Dr. Sebastian Wennig, ZBT - Zentrum für BrennstoffzellenTechnik GmbH, Duisburg for kindly providing the sample material and for the collaboration for this analysis.

Institute for combustion and gas dynamics

The *Nanomaterials synthesis* team investigates the gas-phase synthesis of nanoparticles in combination with materials characterization and processing. The goal is to obtain a better understanding of the synthesis process and thereby make novel processes viable on an industrial scale.

Research in the *Nanoprocessing* group focuses on the dispersion and ink formulation of nanoparticles for their large-scale coating on flexible substrates. The research group is striving for energy applications and sustainable technologies including batteries, fuel cells, and (Opto)electronics.

ZBT - The hydrogen and fuel cell center

ZBT is one of the leading research institutes for fuel cell, hydrogen and energy storage technologies in Europe. Since 2008, ZBT has been working on the further development of innovative and environmentally friendly battery technologies, especially lithium-ion and lithium-sulfur batteries. The focus is set on the development of slurries and electrodes as well as their physical and electrochemical characterization.

Anton Paar

Anton Paar develops, produces and distributes highly accurate laboratory instruments and process measuring systems, and provides custom-tailored automation and robotic solutions. It is the world leader in the measurement of density, concentration and CO_2 and in the field of rheometry.

Measurements & Text

Dr. Sebastian Wennig, Zentrum für BrennstoffzellenTechnik (ZBT) GmbH, Duisburg, GER

Dr. Martin Pfeiler-Deutschmann, Anton Paar GmbH, Graz, AUT

Contact Anton Paar GmbH

Tel: +43 316 257-0

support-nsp@anton-paar.com | www.anton-paar.com

6 References

[1] M. Armand, J.-M. Tarascon, *Nature*, *451 (*7179), **2008**, 652–657.

[2] J. Yang, Y. Xia, *J. Electrochem. Soc.*, *163 (*13), **2016**, A2665-A2672.

[3] Y. Xi, Y. Liu, D. Zhang, S. Jin, R. Zhang, M. Jin, *Solid State Ion.*, *327*, **2018**, 27–31.

[4] J. Hwang, K. Do, H. Ahn, *Chem. Eng. J.*, *406*, **2021**, 126813.

[5] L. Zhu, Y. Chen, C. Wu, R. Chu, J. Zhang, H. Jiang, Y. Zeng, Y. Zhang, H. Guo, *J. Alloys Compd.*, *812*, **2020**, 151848.

[6] B. Long, Y. Zou, Z. Li, Z. Ma, W. Jiang, H. Zou, H. Chen, *ACS Appl. Energy Mater.*, *3 (*6), **2020**, 5572–5580.

[7] R. Gao, J. Tang, X. Yu, S. Tang, K. Ozawa, T. Sasaki, L.-C. Qin, *Nano Energy*, *70*, **2020**, 104444.

[8] L. Ma, J. Meng, Y. Pan, Y.-J. Cheng, Q. Ji, X. Zuo, X. Wang, J. Zhu, Y. Xia, *Langmuir*, *36 (*8), **2020**, 2003–2011.

[9] Z. Li, Y. Zhang, T. Liu, X. Gao, S. Li, M. Ling, C. Liang, J. Zheng, Z. Lin, *Adv. Energy Mater.*, *10 (*20), **2020**, 1903110.

[10] B. Chang, J. Kim, Y. Cho, I. Hwang, M. S. Jung, K. Char, K. T. Lee, K. J. Kim, J. W. Choi, *Adv. Energy Mater.*, *10 (*29), **2020**, 2001069.

[11] D. Zhang, A. Dai, B. Fan, Y. Li, K. Shen, T. Xiao, G. Hou, H. Cao, X. Tao, Y. Tang, *ACS Appl. Mater. Interfaces*, *12 (*28), **2020**, 31542–31551.

[12] K. W. Mu, K. X. Liu, Z. Y. Wang, S. Zanman, Y. H. Yin, X. B. Liu, Y. S. Li, B. Y. Xia, Z. P. Wu, *J. Mater. Chem. A*, *8 (*37), **2020**, 19444–19453.

[13] H. Y. Tran, G. Greco, C. Täubert, M. Wohlfahrt-Mehrens, W. Haselrieder, A. Kwade, *J. Power Sources*, *210*, **2012**, 276–285.

[14] A. Kraytsberg, Y. Ein-Eli, *Adv. Energy Mater.*, *6 (*21), **2016**, 1600655.

[15] R. Dominko, M. Gaberscek, J. Drofenik, M. Bele, S. Pejovnik, J. Jamnik, *J. Power Sources*, *119-121*, **2003**, 770–773.

[16] A. Ponrouch, M. R. Palacín, *J. Power Sources*, *212*, **2012**, 233–246.

[17] R. Wang, H. Mo, S. Li, Y. Gong, B. He, H. Wang, *Sci. Rep.*, *9 (*1), **2019**, 946.

[18] A. Andersson, J. Thomas, *J. Power Sources*, *97-98*, **2001**, 498–502.

[19] N. Ravet, Y. Chouinard, J. F. Magnan, S. Besner, M. Gauthier, M. Armand, *J. Power Sources*, *97-98*, **2001**, 503–507.